



Chemical Characteristics of Particulate Matter and Gaseous Pollutants around Quesna Industrial City, in Monufia Governorate, Egypt

H. M. Nageeb^{1*}, D. F. Slima¹, M. A. Zayed¹, Y. H. Ibrahim²

¹Botany and Microbiology Department, Faculty of Science, Menoufia University, Egypt

²Environment Division, National Research Centre, Dokki, Cairo, Egypt



Abstract

The present study reports characterization of some gaseous and particulate pollutants in three different studied sites around Quesna Industrial City, in Monufia Governorate, Egypt. Samples were collected monthly from December 2018 to November 2019 in all studied sites. Seasonal mean concentrations ($\mu\text{g}/\text{m}^3$) of SO_2 , NO_2 and NH_3 were higher in spring, summer and winter, respectively, with maximum concentrations recorded at site 1 (urban-industrial area). Dust fall concentrations were higher in autumn, with maximum values recorded at site 1 followed by site 3 (traffic-residential area). The monthly mean concentration of dust varied from 17.41 to 221.28 ($\text{g}/\text{m}^3/\text{month}$). Dust fall, have no Air Quality Limit value. However, some countries normally state that when dust fall values exceed 10 g/m^3 per 30 days, the area is considered unclean (polluted). The chemical composition of dust fall including SO_4^{2-} , Cl^- , NH_4^+ and NO_2^- (%) was analyzed for samples collected from the three studied sites. Correlation coefficient values of the relationships between the chemical constituents of collected dust samples indicated that the total soluble and insoluble matter were negatively correlated ($P \leq 0.01$). A significant negative correlation was found between SO_2 and NO_2 at 0.05 significant level for samples collected from semi-residential area.

Keywords: Dust fall, Gaseous pollutants, Industrial pollution, Traffic pollution.

1. Introduction

Air pollution is one of the most important environmental problems in the developing countries[1]. Poor air quality due to air pollutants considered the most recognized environmental problems in urbanized areas around the world. Air Pollution defined as the human introduction into the atmosphere of chemicals, particulate matter or biological materials that cause harm or discomfort to humans, or other living organism or damage the environment. Air pollution is a major problem arising mainly from industrialization [2].

Air pollution occurs when gases, dust particles, fumes (or smoke) or odor are introduced into the atmosphere in a way that makes it harmful to humans, animals and plants. Air pollution threatens the health of humans and other living beings in our planet. It creates smog and acid rain, causing cancer and respiratory diseases, reducing the ozone layer atmosphere and contributing to global warming. In this industrial age, air pollution cannot be completely

eliminated, but steps can be taken to reduce it. The government had developed guidelines for air quality and ordinances to restrict emissions in an effort to control air pollution [3].

The air pollutants emitted from the different industries into the atmosphere are either gaseous or particulates. Over the years there has been a continuous increase in human population, road transportation, vehicular traffic and industries, which has resulted in further increase in the concentration of gaseous and particulate pollutants[4]. Industrialization and the automobiles are responsible for maximum amount of air pollutants [5].

Particulate matter (PM), along with ozone (O_3), nitrogen dioxide (NO_2), sulfur dioxide (SO_2), and carbon monoxide (CO) are the common harmful ambient air pollutants[6]. Atmospheric particulate matter (PM) has received wide attention due to its adverse impacts on human health and the environment[7].

*Corresponding author e-mail: hadeer_nageeb@yahoo.com; (Hadeer Nageeb).

EJCHEM use only: Received date 16 October 2022; revised date 23 December 2022; accepted date 29 January 2023

DOI: 10.21608/EJCHEM.2023.169160.7097

©2023 National Information and Documentation Center (NIDOC)

Dust-fall pollution represents one of the major concerns in Egypt because it significantly contributes to environmental damage and health problems [8]–[11]. It represents air particulate matter containing a mixture of organic and inorganic pollutants. After temporary suspension in air, dust has the capability to settle down. Generally, dust originates from natural and anthropogenic sources such as soils, surrounding desert environment, industrial wastes, traffic congestion, incomplete fuel combustion in domestic heating, industrial plants, and vehicular exhausts. Soil dust represents major constituents in the dust-fall samples. Physical, chemical, and mineralogical characterization of the dust-fall samples are essential to understanding the influence of dust in the environment and in human health [10].

PM results from natural and anthropogenic processes, such as wind erosion, volcanic eruptions, marine salt formations, industrial production, coal combustion and vehicle emissions. PM is a complex mixture of suspended solid and liquid particles with different physical and chemical properties, originating from natural and anthropogenic sources. Organic matter, sulphate, nitrate, ammonium and elemental carbon are the main PM contributors. Organic carbon and elemental carbon originate from combustion processes; primary organic carbon arises from combustion, geological and natural sources, while secondary organic carbon is formed when the atmospheric oxidation products of Volatile Organic Compounds (VOCs) undergo gas–particle transfer. Elemental carbon is essentially a primary pollutant emitted during the incomplete combustion of fossil and biomass carbonaceous fuels [12].

Particulate matter (PM) pollution is a serious health issue throughout the world, exacerbating a wide range of respiratory and vascular illnesses in urban areas [13]. PM results from natural and anthropogenic processes, such as wind erosion, volcanic eruptions, marine salt formations, industrial production, coal combustion and vehicle emissions. The size of the PM is an essential characteristic because it determines its behavior and toxicity. Smaller particles such as PM 2.5 (fine particulate matter with an aerodynamic diameter less than 2.5 μm) or UFP (ultrafine particles with an aerodynamic diameter less than 0.1 μm) can more easily penetrate the pulmonary alveoli and hence are more harmful to human health [14].

Long-term exposure to PM has more negative impact on human health compared to high levels of daily (short-term) exposure [15]. Heavy metals deposit on the finest fraction of particulate matter. Many studies on the elemental composition of PM collected from air in different world regions and months confirmed the presence of following heavy

metals Ti, Fe, Pb, Mn, Cr, Mn, Cu, Cd, V, Ni, Mo, As, Co, Sb and Hg [16].

Earlier studies on PM_{2.5} in Lanzhou investigated the effect of topographic and meteorological conditions and potential sources and transport pathways causing the accumulation of PM_{2.5} [17], [18]. More recent studies analyzed the chemical characteristics of PM_{2.5} focusing on trace elements, OC and EC, and water soluble inorganic species [19]–[21].

Levels of pollutants in the air have decreased over the past decades, but in many urban areas, the levels of particulate matter (PM), ground-level ozone (O₃), nitrogen dioxide (NO₂), and volatile organic compounds (VOC) still high enough to cause serious human health problems. Most of such air pollutants arise from road traffic and energy production. Industry, power stations, transportation, agriculture, and waste management may also contribute to air pollution [22].

The present study aims to evaluate the chemical characteristics of particulate matter (dust) and gaseous pollutants around Quesna Industrial City, in Monufia Governorate, Egypt, during December 2018 - November 2019.

Material and method

I-Climatic factors

Meteorological data during the sampling period obtained from <http://www.wunderground.com>. Table 1 showed the average of prevailing climatic conditions {temperature (°C), dew point (°C), relative humidity (%), wind speed (mph) and Precipitation (inch)} for Quesna city during the period 2018-2020.

II-Geographical locations of study

In this study, seasonal variations of major groups of dust-fall chemical components were characterized. In addition, we investigated the air quality in terms of gases pollutants as SO₂, NO₂ and NH₃. This study was carried out on three sites, which are:

site1: {an urban–industrial area} located in the industrial sector (Mubarak industrial city) inside Quesna city (30°32'41.6"N 31°10'34.7"E), which is a city in Southeast of Monufia Governorate, Egypt as illustrated in map 1. Quesna industrial city has an area of 203.9 Km². Hundreds of various size factories (plants) located in this area beside the high-density residential activities. However, the main sources of pollution are electronics, home appliances, food industries, furniture, spinning, weaving, Glue industry, ceramic, glass and metallurgical industries. The various industrial activities in Mubarak industrial city will no doubt contaminate its

own atmosphere and surrounding area by different **Site 2: {Semi-residential area}** located at the Faculty of Science, Menoufia University, (N36°02'47.38", E103°49'50.87"). The site is located in a residential and commercial area without nearby industrial emission sources (map 1). This building has also been used for monitoring of ambient air pollutants such as concentrations of dust-fall, SO₂, NO₂, and NH₃.

particulates and gaseous pollutants.

Site 3: Traffic road {traffic-residential area} which located at the rood between El Bajour and Shebin El Kom cities of Menoufia governorate, Egypt (30°26'25.3"N 31°02'06.5"E). All samples were collected monthly at the same time from 1/12/2018 to 31/11/2019.



Map 1: The studied locations (site 1, 2 and 3) where the air samples were collected

1. Determination of deposited matter

1.1. Sampling of total dust-fall

Dust collectors were used for collecting dust-fall. The collectors consist of cylindrical glass beaker 17 cm height and 9 cm diameter. The beaker was half filled with distilled water and mounted on iron tripods at height of 50 cm above roof level to avoid that collection of re-suspended dust. Dust jars were collected at the beginning of each month. The monthly rate of deposition from the different sites were calculated as gm.m².month; and then analyzed for water-soluble and in soluble fractions [17].

1.2. Chemical analysis of dust-fall

Jar contents were transferred quantitatively to dry clean pre-weighted beaker using successive washing with distilled water until the inside of the jar is cleaned. Then the beaker was dried to constant weight in electrical oven at 60-80°C, the difference in weights represent the amount of dust-fall and expressed as gm.m².month [18].

1.2.1. Determination of water soluble matter

After determination of dust-fall, the beaker content was re-suspended in 200 mL distilled water

and filtered through ash-less filter paper (What-man-filter paper no. 42). After that, the filtrate was divided into 8 equal portions (each equalled 25 mL). One of these portions was evaporated in dry clean weighted 100 mL beaker over water bath until dryness [18]. The excess in weight of the beaker was multiplied by 8 to give the amount of total soluble matter and then expressed as (%) the remaining portions of the filtrate were used for determination of (sulphate, ammonium, chlorides, and nitrites).

1.2.1.1. Determination of chlorides (Cl⁻)

Chlorides were determined by using turbid-metric measurement of the precipitated silver chloride in the samples [23]. A portion of filtrate (25 mL) was transferred to 100 mL flask, and then 5 mL of 0.01 N silver nitrate dissolved in diluted nitric acid (1:5) was added. After standing for 5 minutes, precipitation of silver chloride formed. The turbidity measured at 560 nm using a spectrophotometer (spectroUVS-2700/UVS-2800). Different concentrations of sodium chloride (NaCl) were used to prepare standard curve.

1.2.1.2. Determination of sulphate (SO₄⁻²)

Sulphate was determined as barium sulphate at 500 nm [24]. Another portion of filtrate (25 mL) was transferred to 100 mL flask, then 1 mL of 10 N HCL

was added to the sample and mixed with 4 mL glycerol alcohol solution (1 glycerol:2 alcohol 95%). A spoon full of $\text{BaCl}_2 \cdot 2\text{H}_2\text{O}$ crystals added. Then the mixture allowed to stand for 40 min. standard curve of different concentrations of sulphate were prepared using Na_2SO_4 .

1.2.1.3. Determination of ammonium (NH_4^+)

Nessler's method [25], [26] was used for determination of ammonium salts in water soluble matter. Another portion of filtrate (25 mL) was transferred to 100 mL flask, then 4 mL of Nessler's reagent was added and mixed. The developed yellow color was determined colorimetrically at 460 nm with reference to blank.

1.2.1.4. Determination of nitrates (NO_3^-)

Nitrates were determined by the method described by [27]. 25 mL of filtrate was transferred into 100 mL beaker. 1 mL of sodium salicylate was added and evaporated on water bath until dryness then cooled. 2 mL of concentrated H_2SO_4 were added to the beaker containing the samples and left for 10 min. In addition, 15 mL distilled water and 15 mL NaOH mixture were added, then allowed to stand for 10 min. the samples were measured at 420 nm by using spectrophotometer (spectroUVS-2700/uvs-2800).

1.2.1.5. Determination of heavy metals (Pb and Cd)

Heavy metals (Pb and Cd) were determined in 25 mL of filtrate using atomic absorption spectrophotometer, (model Perkin Elmer, 2380A Analyst 100).

1.2.2. Determination of water insoluble matter

The total insoluble matter calculated by subtracting the weight of soluble matter from total weight of deposited matter (dust-fall).

1.2.2.1. Ash fraction

The filter paper containing the insoluble fraction was transferred to pre-weighed crucible and ignited in muffle furnace at 600°C for 8 h. The crucibles were cooled in a desiccator and weighed. The difference in weight represents the ash fraction [24].

2. Measurement of gaseous pollutants

2.1. Determination of SO_2

SO_2 in ambient air was determined by the method described by [22] as following:

Reagent

a) Absorbing reagent 0.1M sodium tetrachloromercurate (mercuric chloride 27.2g and sodium chloride 11.7 g were dissolved in 1 L distilled water).

b) Acid-bleached 0.04% pararosaniline hydrochloride (0.2 g pararosaniline hydrochloride dissolved in 100 mL distilled water and left for 48 h then filtrated. 20 mL of this solution was transferred into 100 mL volumetric flask. 6 mL of conc. HCL was added; the solution was allowed to stand for 5 min. and diluted to mark with dis. H_2O).

c) 0.2% Formaldehyde (5 mL of 40% formaldehyde diluted to 1L with dis H_2O).

d) Standard solution (sodium metabisulfite, 0.64 g) was dissolved in 1L dis. H_2O (assay 65.6 as SO_2). This yield a solution of approximately 0.4 mg/ mL as SO_2 , this solution was standardized by titration with standard 0.01 N I_2 with starch as indicator. Then series of different concentrations were prepared from standard solution.

i. sampling

SO_2 in ambient air was determined by the method described by [28]. Air was aspirated (1 L/min for 24 h) through a glass bubbler sampler containing 50 mL of absorbing solution.

Addition of acid bleached pararosaniline and formaldehyde to the complex ion produce red-purple pararosaniline methyl sulphonic acid, which is determined spectrophotometrically at 560 nm.

ii. Analytical analysis

The collected samples transferred into a flask, and then 5 mL of formaldehyde and 5 mL of acid bleached pararosaniline were added. The blank prepared by the same manner using equal volume of unexposed sample of sodium tetrachloromercurate solution. The mixture was allowed to stand for 20 min. for maximum color development, and the absorbance of samples were measured at 560 nm. The concentration of SO_2 was calculated from standard curve (expressed as $\mu\text{g}/\text{m}^3$).

2.2. Determination of NO_2

NO_2 in ambient air was determined by the sulphanilamide diazotization method according to [19]

Reagent

a) Absorbing reagent: 4 g sodium hydroxide dissolved in 1L of distilled water (0.1 N), 1 mL of butanol added to this solution to increase foaming and assist in trapping the nitrogen dioxide.

b) Diazotizing reagent: 20 g of sulphanilamide dissolved in 1L of distilled water containing 50 mL of phosphoric acid (85%).

c) (NEDA) n-(1-naphthyl)ethylenediamine dihydrochloride: 1 gm of NEDA dissolved in 1L of distilled water.

d) Formaldehyde (0.2%): 5 mL of 40% formaldehyde diluted to 1L with dis H_2O .

e)H₂O₂ (hydrogen peroxide): 0.2 mL of 30% H₂O₂ diluted to 250 mL with distilled water.

i. sampling

Air was aspirated (1 L/min for 1h) through a glass bubbler sampler contain 50 mL of absorbing solution (0.1 N sodium hydroxide).

ii. Analytical analysis

The collected samples transferred into a flask, and then 1 mL of H₂O₂ added and mixed to oxidize the dissolved SO₂ to SO₄. 10 mL of diazotizing reagent added and then 1.4 mL of NED added. The blank prepared by the same manner using unexposed absorbing reagent. The mixture allowed standing for 10 min. until the color developed, and the absorbance of samples measured at 550 nm. The concentration of NO₂ calculated from standard curve (expressed as µg/m³ of air).

2.3. Determination of NH₃

Results

a) Climate

The study area characterized by hot and dry summer, rare rainfall during winter and bright sunshine through the year. The study area was characterized by 23.24°C, while the average of dew

NH₃ in ambient air was determined according to [26]. The air samples were collected by aspirating air (1L/min for 24 h) through a glass bubbler sampler containing 50 mL of absorbing solution (diluted H₂SO₄). The solution treated with Nessler's reagent and the intensity of the produced color measured at 460 nm. The concentration of ammonia in the solution determined by standard curve with different concentrations of ammonium chloride solutions.

Statistical analysis

Statistical analysis of the results were analyzed using T-test (2-tailed) and the results considered significant when $P \leq 0.05$. In addition, correlation was calculated between samples using Pearson Correlation.

point is 11.70°C; relative humidity was 52.18% (Table 1). The dominant wind directions are from southeast in summer and east in winter with an average speed of 11.08 Km/h.

Table 1: Meteorological data (averaged) for Quesna city from December 2018 to November 2019

Month	Temperature	Dew Point	Humidity	Wind Speed	Precipitation
Dec-18	16.684	8.032	58.11	8.535	0
Jan-19	13.99	1.548	46.18	10.584	0
Feb-19	15.72	5.098	52.51	8.343	0
Mar-19	17.713	7.506	55.14	10.119	0
Apr-19	21.013	8.26	48.23	9.38	0
May-19	27.435	9.545	38.15	9.713	0
Jun-19	29.577	16.94	49.63	15.14	0
Jul-19	30.271	18.59	52.78	12.597	0
Aug-19	30.345	18.86	54.07	11.926	0
Sep-19	27.93	18.28	57.93	13.303	0
Oct-19	25.897	16.48	59.17	12.339	0
Nov-19	22.29	11.26	54.23	11.013	0
Annual Mean	23.24	11.70	52.18	11.08	0

b) Dust-fall

• Total Dust-fall

The dust-fall measurement is an indication of the quantity of large particles. Dust precipitation was monthly collected using Dust collectors and expressed as g/m³ /month. T-test was used for comparing the obtained results. Tables 2, 4 and 6, and figure 2-4 show the rates of total deposited matter

over the investigated sites during the period of study. The annual means of Dust were 65.74±60.52, 72.67±17.46 and 78.28±8.45 g/m³/month for sites 1, 2 and 3 respectively. The highest rate of dust-fall deposition was recorded during month of October (221.28 g/m³/month) for site 1 (industrial area), November (93.91 g/m³/month) for site 2 and October (99.45 g/m³/month) for site 3. Tables (2, 4

and 6) shows that the rate of dust deposition was higher in autumn season followed by spring season for sites 1 and 3 during the period of study, while in site 2 the highest amount of dust deposited in autumn followed by winter season.

Chemical Composition of Dust-fall

b) Water Soluble Fraction of Dust-fall

The concentration of chemical constituents (expressed as %) for seasonal and annual means of the total water-soluble matter (TSM) in total deposits shown in tables 2, 4, 6 and figure 2-4 B. Moreover, concentration of TSM varied from one month to another with a slightly higher concentration during autumn ($31.66 \pm 3.71\%$ for site 1) and winter and autumn for site 3 (was about 26% in both seasons). In addition, the highest concentrations of TSM were 34.67, 32.33, and 33.4 in November, August and June months for sites 1, 2 and 3 respectively. These months are characterized by passage of sand storms over Egyptian countries and carry with them desert sands that contains in soluble compounds.

1. Sulphates in Total Dust-fall:

The results illustrate that the mean concentration of sulphates in the different studied locations recorded the highest concentrations during summer season for site 1 ($10.25 \pm 4.04\%$), during spring ($4.56 \pm 1.19\%$) for site 2 and during winter ($3.31 \pm 0.42\%$) for site 3 figures 2-4E.

2. Chlorides in Total Dust-fall:

Airborne chlorides are the suspended salt and gaseous content present in the atmosphere. For example, large quantities of chlorine are released

from water purification plants, evaporated ocean spray as sea salt (sodium chloride) particles. Volcanoes can emit large quantities of hydrogen chloride, but this gas is rapidly converted to hydrochloric acid, which dissolves in rainwater and does not reach the stratosphere. Figures 2-4 f show the average monthly percentage of chlorides in total dust-fall at the different studied sites.

The results showed a relatively higher value of chlorides during summer and autumn seasons for site 1 and 2. The mean seasonal percentage of chlorides varied between 0.13 ± 0.11 and 0.44 ± 0.29 , 0.39 ± 0.34 and 0.63 ± 0.82 for autumn and summer seasons for samples collected from site 1 and 2, respectively. While, it varied between 0.17 ± 0.11 and 0.64 ± 0.41 during winter and autumn seasons for samples collected from site 3.

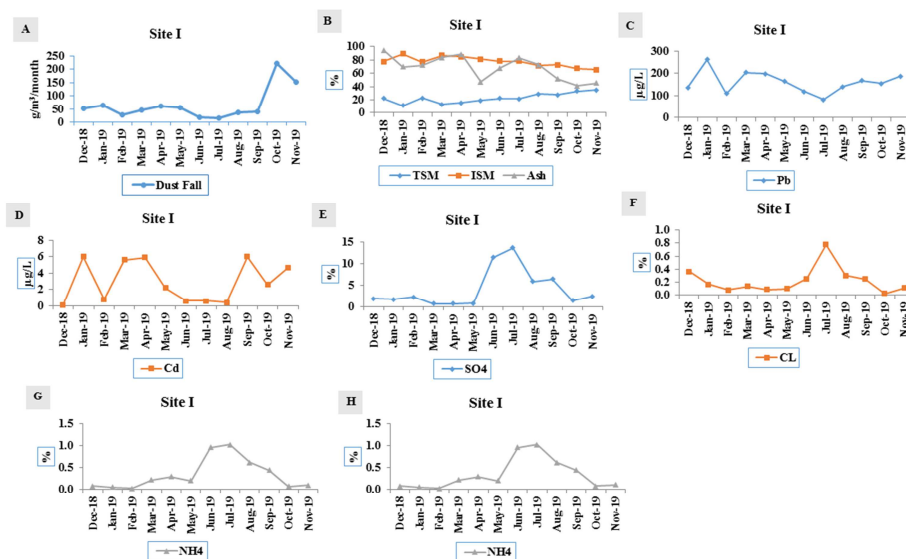


Figure 1: Chemical analysis of dust samples Collected from site (1)

Table 2: Chemical Analysis Of Dust Samples Collected From Site (1)

Season	Month	TSM	INS	Dust fall	Ash	Pb	Cd	SO ₄	CL	NH ₄	NO ₃
Winter	Dec-18	22.24	77.76	51.82	94.67	137	0.11	1.85	0.36	0.08	0.27
	Jan-19	11.05	88.95	63.74	69.55	263	5.99	1.63	0.17	0.06	0.18
	Feb-19	22.85	77.15	28.59	71.96	109	0.81	2.16	0.08	0.03	0.49
	Mean ±SD	18.71±6.6	81.29±6.6	48.05±17.9	78.73±13.8	169.67±82.1	2.3±3.2	1.88±0.27	0.2±0.15	0.06±0.03	0.31±0.16
Spring	Mar-19	13.32	86.68	46.82	83.27	204	5.59	0.56	0.13	0.22	0.24
	Apr-19	15.5	84.5	62.04	88.13	198	5.89	0.58	0.09	0.3	0.25
	May-19	19.04	80.96	53.96	47.29	164	2.19	0.67	0.1	0.2	0.16
	Mean ±SD	15.95±2.9	84.05±2.9	54.27±7.6	72.9±22.3	188.67±21.6	4.56±2.1	0.6±0.06	0.11±0.02	0.24±0.05	0.21±0.05
Summer	Jun-19	21.92	78.08	17.41	67.61	119	0.61	11.38	0.25	0.96	0.22
	Jul-19	21.71	78.29	15.21	83.2	82.3	0.61	13.61	0.78	1.03	0.32
	Aug-19	28.56	71.44	37.21	72.55	140	0.39	5.77	0.3	0.62	0.1
	Mean ±SD	24.06±3.9	75.94±3.9	23.28±12.1	74.46±7.9	113.77±29.2	0.54±0.1	10.25±4.04	0.44±0.3	0.87±0.2	0.22±0.1
Autumn	Sep-19	27.51	72.49	38.15	51.56	167	5.99	6.38	0.25	0.44	0.1
	Oct-19	32.8	67.2	221.28	40.99	155	2.59	1.33	0.02	0.08	0.03
	Nov-19	34.67	65.33	152.62	45.27	188	4.7	2.39	0.11	0.11	0.06
	Mean ±SD	31.66±3.7	68.34±3.7	137.35±92.5	45.94±5.3	170±16.7	4.43±1.7	3.37±2.7	0.13±0.1	0.21±0.2	0.07±0.04
Annual Mean		22.6±7.4	77.4±7.4	65.74±60.5	68.01±18	160.53±48.7	2.96±2.5	4.03±4.4	0.22±0.2	0.34±0.4	0.2±0.1
T-Test		2.70E-04	3.70E-11	1.06E-02	6.28E-07	4.27E-07	1.69E-01	6.10E-05	5.79E-21	2.65E-18	3.23E-23

Table 3: Correlation Coefficient Values Of The Relationships Between The Chemical Constituents Of Dust Samples Collected From Site (1)

Item	TSM	INS	Dust	Ash	Pb	Cd	SO ₄	CL	NH ₄	NO ₃
TSM	1	-1.000**	0.546	-.587*	-0.403	-0.281	0.162	-0.036	0.03	-0.48
INS	-1.000**	1	-0.546	.587*	0.403	0.281	-0.162	0.036	-0.03	0.48
dust	0.546	-0.546	1	-.604*	0.275	0.228	-0.441	-0.492	-0.499	-.616*
Ash	-.587*	.587*	-.604*	1	-0.122	-0.184	0.115	0.444	0.199	.643*
Pb	-0.403	0.403	0.275	-0.122	1	.836**	-.633*	-0.54	-0.552	-0.394
Cd	-0.281	0.281	0.228	-0.184	.836**	1	-0.437	-0.43	-0.372	-0.332
SO ₄	0.162	-0.162	-0.441	0.115	-.633*	-0.437	1	.787**	.932**	0.122
CL	-0.036	0.036	-0.492	0.444	-0.54	-0.43	.787**	1	.717**	0.25
NH ₄	0.03	-0.03	-0.499	0.199	-0.552	-0.372	.932**	.717**	1	0.061
NO ₃	-0.48	0.48	-.616*	.643*	-0.394	-0.332	0.122	0.25	0.061	1

*. Correlation is significant at the 0.05 level (2-tailed).
 **. Correlation is significant at the 0.01 level (2-tailed).

Table 4: Chemical Analysis of Dust Samples Collected From Site (2)

Season	Month	TSM	INS	Dust	Ash	Pb	Cd	SO ₄	CL	NH ₄	NO ₃
winter	Dec-18	13.25	86.75	58.73	74.86	1000	3.39	2.18	0.13	0.44	0.1
	Jan-19	12.01	87.99	82.51	54.31	317.5	1.49	2.48	0.09	0.29	0.04
	Feb-19	29.74	70.26	76.25	29.62	300	0.59	4.03	0.16	0.08	0.08
Mean± SD		18.33±9.9	81.67±9.9	72.5±12.33	52.93±22.65	539.17±399.19	1.82±1.43	2.9±0.99	0.12±0.04	0.27±0.18	0.07±0.03
spring	Mar-19	31.81	68.19	64.6	76.72	229	3.39	4.6	0.15	0.38	0.05
	Apr-19	26.4	73.6	92.03	68.2	272	3.39	3.34	0.22	0.05	0.14
	May-19	21.22	78.78	55.69	70.77	160.8	0.11	5.73	0.27	0.39	0.13
Mean± SD		26.47±5.3	73.53±5.3	70.77±18.94	71.9±4.37	220.6±56.07	2.3±1.89	4.56±1.19	0.21±0.06	0.27±0.19	0.11±0.05
summer	Jun-19	28.12	71.88	38.37	33.33	196.9	2.69	1.22	0.24	0.44	0.13
	Jul-19	25.02	74.98	70.11	12.58	230	0.51	3.36	1.57	0.23	0.1
	Aug-19	32.33	67.67	88.07	32.36	93.5	0.71	0.16	0.08	0.17	0.12
Mean± SD		28.49±3.67	71.51±3.67	65.52±25.17	26.09±11.71	173.47±71.2	1.3±1.21	1.58±1.63	0.63±0.82	0.28±0.14	0.12±0.01
autumn	Sep-19	19.16	80.84	61.28	67.21	118.8	1.29	0.42	0.16	0.25	0.29
	Oct-19	24.81	75.19	90.51	62.6	100.7	4	0.97	0.23	0.17	0.06
	Nov-19	27.35	72.65	93.91	66.16	111.4	6.1	3.89	0.77	1.38	0.13
Mean± SD		23.78±4.19	76.22±4.19	81.9±17.94	65.33±2.41	110.3±9.1	3.8±2.41	1.76±1.87	0.39±0.34	0.6±0.68	0.16±0.12
Annual Mean		24.27±6.67	75.73±6.67	72.67±17.46	54.06±21.4	260.88±245.59	2.31±1.81	2.7±1.76	0.34±0.43	0.35±0.35	0.11±0.07
T-Test		1.24E-04	9.00E-10	1.12E-07	2.92E-05	4.88E-03	7.14E-01	1.36E-09	2.43E-17	2.65E-18	2.28E-26

Table 5: Correlation Coefficient Values Of The Relationships Between The Chemical Constituents Of Dust Samples Collected At Site (2)

Item	TSM	INS	Dust	Ash	Pb	Cd	SO ₄	CL	NH ₄	NO ₃
TSM	1	-1.000**	-0.270	-0.152	-0.575	-0.176	0.224	0.311	-0.085	0.557
INS	-1.000**	1	0.270	0.152	0.575	0.176	-0.224	-0.311	0.085	-0.557
dust	-0.270	0.270	1	0.043	-0.258	0.511	-0.042	0.067	0.071	-0.238
Ash	-0.152	0.152	0.043	1	0.232	0.258	0.211	-0.481	0.274	0.119
Pb	-0.575	0.575	-0.258	0.232	1	-0.256	0.047	-0.149	-0.039	-0.212
Cd	-0.176	0.176	0.511	0.258	-0.256	1	0.007	0.214	.723**	-0.099
SO ₄	0.224	-0.224	-0.042	0.211	0.047	0.007	1	0.242	0.236	-0.317
CL	0.311	-0.311	0.067	-0.481	-0.149	0.214	0.242	1	0.270	0.012
NH ₄	-0.085	0.085	0.071	0.274	-0.039	.723**	0.236	0.270	1	0.040
NO ₃	0.557	-0.557	-0.238	0.119	-0.212	-0.099	-0.317	0.012	0.040	1

**. Correlation is significant at the 0.01 level (2-tailed).

Table 6: Chemical Analysis Of Dust Samples Collected From Site 3

Season	Month	TSM	INS	Dust	Ash	Pb	Cd	SO ₄	CL	NH ₄	NO ₃
Winter	Dec-18	29.86	70.14	75.21	19.58	210.8	3.59	2.83	0.09	0.07	0.22
	Jan-19	26.96	73.04	70.51	12.68	104.8	0.79	3.6	0.12	0.08	0.09
	Feb-19	22.17	77.83	78.46	21.09	114.6	0.49	3.51	0.29	0.05	0.12
Mean± SD		26.33±3.88	73.67 ±3.88	74.73±3.99	17.79±4.48	143.4±58.58	1.62±1.71	3.31±0.42	0.17±0.11	0.06±0.01	0.14±0.07
spring	Mar-19	24.74	75.26	79.81	18.66	134	0.21	3.04	0.09	0.32	0.03
	Apr-19	26.42	73.58	75.83	14.67	112.7	0.79	3.04	0.08	0.29	0.07
	May-19	0.44	99.56	82.57	12.97	144	0.41	0.54	0.13	0.18	0.07
Mean± SD		17.2±14.54	82.8±14.54	79.4±3.39	15.43±2.92	130.23±15.99	0.47±0.29	2.21±1.44	0.1±0.02	0.27±0.07	0.06±0.02
summer	Jun-19	33.4	66.6	78.9	18.82	117	0.29	0.49	0.13	0.19	0.2
	Jul-19	6.09	93.91	74.7	15.67	127.9	2.89	0.62	0.17	0.2	0.13
	Aug-19	33.31	66.69	69.41	8.48	71.8	0.41	0.79	0.16	0.21	0.25
Mean± SD		24.26±15.74	75.74±15.74	74.33±4.75	14.32±5.3	105.57±29.75	1.2±1.47	0.63±0.15	0.15±0.02	0.2±0.01	0.2±0.06
autumn	Sep-19	27.94	72.06	65.41	29.78	69	0.3	1.59	0.16	0.22	0.26
	Oct-19	28.34	71.66	99.45	23.56	93.5	3.9	2.38	0.84	0.2	0.12
	Nov-19	21.98	78.02	89.15	19.55	161	4.6	3.25	0.91	0.19	0.14
Mean± SD		26.09±3.56	73.91±3.56	84.67±17.46	24.29±5.16	107.83±47.65	2.93±2.31	2.41±0.83	0.64±0.41	0.2±0.02	0.17±0.08
Annual Mean		23.47±9.39	76.53±9.39	78.28±8.45	17.96±5.24	121.76±36.06	1.56±1.59	2.14±1.19	0.26±0.27	0.18±0.09	0.14±0.08
T-test		2.67E-28	1.10E-26	4.61E-11	3.62E-03	1.70E-05	4.69E-09	1.79E-11	3.08E-19	3.24E-25	8.44E-26

Table 7: Correlation Coefficient Values Of The Relationships Between The Chemical Constituents Of Dust Samples Collected At Site (3)

Item	TSM	INS	Dust-fall	Ash	Pb	Cd	SO ₄	CL	NH ₄	NO ₃
TSM	1	-.588*	0.169	0.270	-0.130	-0.153	0.353	0.279	0.004	0.336
INS	-.588*	1	.698*	-0.050	0.253	0.032	-0.128	0.442	0.068	-.586*
Dust-fall	0.169	.698*	1	0.179	0.386	-0.229	0.156	.786**	0.086	-0.416
Ash	0.270	-0.050	0.179	1	0.557	0.230	0.192	0.328	-0.002	0.249
Pb	-0.130	0.253	0.386	0.557	1	.687*	0.151	-0.303	-0.276	0.006
Cd	-0.153	0.032	-0.229	0.230	.687*	1	-0.001	-0.113	-0.339	0.337
SO ₄	0.353	-0.128	0.156	0.192	0.151	-0.001	1	0.254	-0.238	-0.388
CL	0.279	0.442	.786**	0.328	-0.303	-0.113	0.254	1	-0.024	-0.048
NH ₄	0.004	0.068	0.086	-0.002	-0.276	-0.339	-0.238	-0.024	1	-0.248
NO ₃	0.336	-.586*	-0.416	0.249	0.006	0.337	-0.388	-0.048	-0.248	1
*. Correlation is significant at the 0.05 level (2-tailed). **. Correlation is significant at the 0.01 level (2-tailed).										

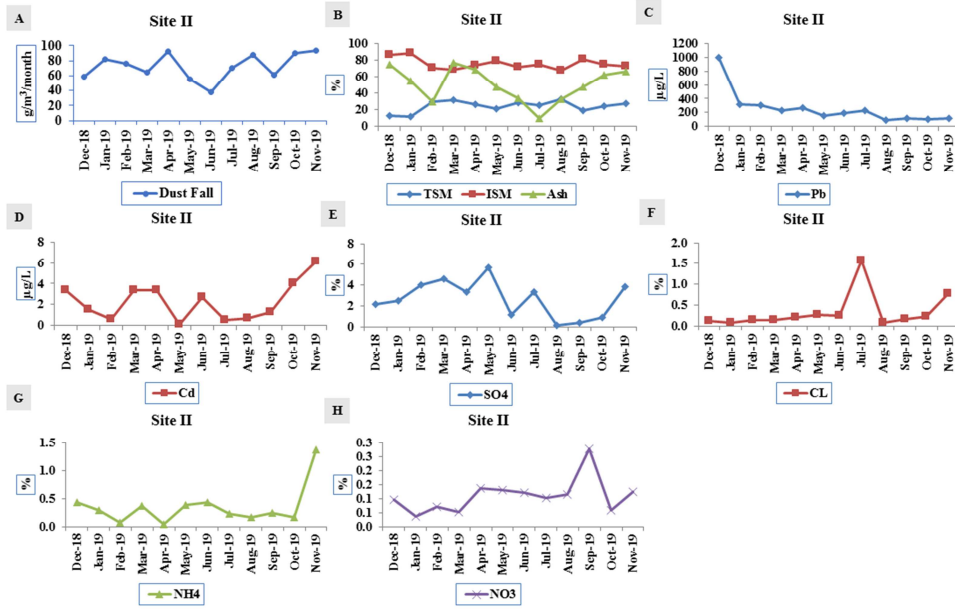


Figure 2: Monthly Means For Chemical Composition Of Dust Samples Collected From Site (2)

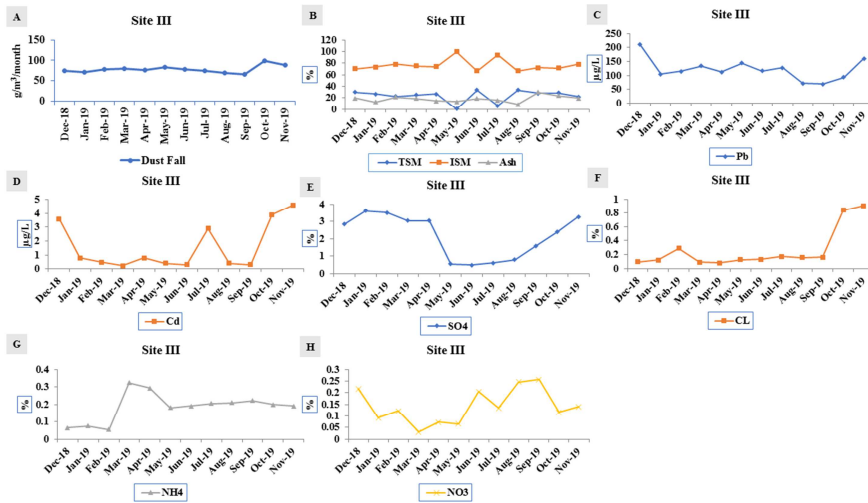


Figure 3: Monthly Means For Chemical Composition Of Dust Samples Collected From Site (3)

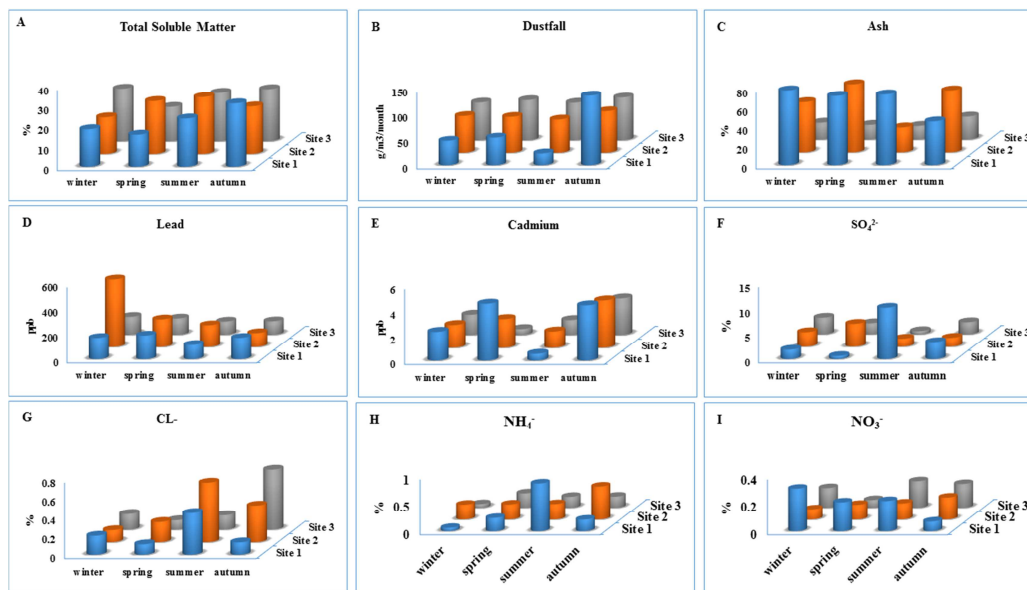


Figure 4: Seasonal Means for Chemical Composition Of Dust Samples Collected From Different Studied Sites

Correlation coefficient values of the relationships between the chemical constituents of dust samples collected at site 1 (table 3), indicated that the total soluble and insoluble matter were negatively correlated ($P \leq 0.01$). In addition, the amount of dust-fall deposited in this site was negatively correlated with ash and nitrates contents at $P \leq 0.05$ significant level. Moreover, the ash content was positively correlated with insoluble matter and nitrates content at the 0.05 significant level. The lead and cadmium contents were positively correlated at the 0.01 significant levels. The sulphate, chlorine and ammonium were positively correlated at 0.01 significant level. Moreover, correlation coefficient values of the relationships between the chemical constituents of dust samples collected at site 2 (table 5) illustrated that there were no significant correlation between the studied chemical components except for TSM and ISM, Cd and NH_4 (at 0.01 significant level). While for site 3 it was found that the amount of dust was positively correlation with INS and Cl^- (table 7). Additionally, total soluble matter was negatively correlation with INS and NO_3^- . The lead and cadmium contents were positively correlated at $P \leq 0.05$.

c) Gaseous Air Pollutants:

Gaseous pollutants monitored in the investigated area atmosphere are SO_2 , NO_2 and NH_3 (expressed as $\mu\text{g}/\text{m}^3$) table (8-10). These are the major gaseous pollutants in industrial and urban areas.

1. Sulphur Dioxide (SO_2):

Concentrations of SO_2 were measured in the three studied sites and the results revealed that the annual

mean concentration of 50.9 ± 15.6 , 15.3 ± 8.6 and 14 ± 3 $\mu\text{g}/\text{m}^3$ were detected in the atmosphere of sites 1, 2 and 3 respectively. The maximum monthly concentrations of 73, 36 and 21 were detected in the atmosphere of the same sites in September, January and October during the period of study. The maximum SO_2 concentrations of 61.0 ± 11.5 , 26.7 ± 10.7 and 16.3 ± 4.5 were recorded in the seasons of autumn, winter and autumn of investigated sites 1, 2 and 3 respectively. The seasonal average concentration of SO_2 of the present study is represented graphically in figure 5A. The higher levels of SO_2 were recorded in winter and autumn seasons and lower concentrations were recorded in summer except site 1.

2. Nitrogen Dioxide (NO_2):

Tables 8-10 summarize the NO_2 concentration in the investigated sites during the period of study. The annual mean concentration of 49.6 ± 19.4 , 31.6 ± 14.8 and 31 ± 16.7 $\mu\text{g}/\text{m}^3$ were detected in the atmosphere of sites 1, 2 and 3 respectively. The maximum monthly concentrations of 90, 55 and 60 were detected in the atmosphere of the same sites in August, June and July during the period of study. The maximum NO_2 concentrations of 61.0 ± 11.5 , 38 ± 10.8 and 50 ± 13.2 were recorded in the seasons of summer, autumn and summer of investigated sites 1, 2 and 3 respectively. The seasonal average concentration of NO_2 of the present study are represented graphically in figure 5B. The maximum seasonal concentrations of NO_2 were recorded in summer and autumn seasons additionally, the highest

concentration of NO₂ was recorded in site 1 followed by site 3.

3. Ammonia (NH₃):

High concentrations of ammonia were recorded in this study in samples collected at the industrial sector of Quesna Industrial City (site 1). The annual mean concentration of 50.3±8.6, 27.8±10.7 and 32.6±13.3 μg/m³ were detected in the atmosphere of sites 1, 2 and 3 respectively. The maximum seasonal mean concentration concentrations of 55.0±5, 40.7±4 and 49.7±5.5 were recorded in the seasons of summer

for site 1, spring of investigated sites 2 and 3, while the minimum seasonal mean concentration of 47.7±6.8, 19±3.6 and 22±9.2 were recorded in autumn of all studied sites. The maximum monthly concentrations of 60, 42 and 50 were detected in the atmosphere of the studied sites respectively during the period of study. The seasonal average concentration of NH₃ of the present study is represented graphically in figure 5C. A significant negative correlation was found between SO₂ and NO₂ at 0.05 significant level for samples collected from site 2.

Table 8: Chemical Analysis of Gaseous Air Pollutants Pollutant at Site (1).

Season	Month	SO ₂	NO ₂	NH ₃
Winter	Dec-18	35	30	60
	Jan-19	26	35	55
	Feb-19	46	40	45
Av ± SD		35.7±10	35.0±5	53.3±7.6
Spring	Mar-19	53	35	60
	Apr-19	60	30	35
	May-19	55	30	40
Av ± SD		56.0±3.6	31.7±2.9	45.0±13.2
Summer	Jun-19	40	55	50
	Jul-19	35	70	60
	Aug-19	78	90	55
Av ± SD		51.0±23.5	71.7±17.6	55.0±5
Autumn	Sep-19	73	65	53
	Oct-19	60	55	50
	Nov-19	50	60	40
Av ± SD		61.0±11.5	60.0±5	47.7±6.8
Annual mean ± SD		50.9±15.6	49.6±19.4	50.3±8.6
T-Test Sig. (2-tailed)		3.00E-06	3.30E-05	8.30E-09

Table 9): Chemical Analysis of Gaseous Air Pollutant at Site (2).

Season	month	SO ₂	NO ₂	NH ₃
Winter	Dec-18	15	20	25
	Jan-19	36	25	20
	Feb-19	29	30	15
Av ± SD		26.7±10.7	25±5	20±5
Spring	Mar-19	15	29	37
	Apr-19	12	35	45
	May-19	10	50	40
Av ± SD		12.3±2.5	38±10.8	40.7±4
Summer	Jun-19	8	55	42
	Jul-19	9	30	30
	Aug-19	15	10	22
Av ± SD		10.7±3.8	31.7±22.5	31.3±10.1
Autumn	Sep-19	10	9	15
	Oct-19	10	49	22
	Nov-19	15	37	20
Av ± SD		11.7±2.9	31.7±20.5	19±3.6
Annual mean ± SD		15.3±8.6	31.6±14.8	27.8±10.7
T-Test Sig. (2-tailed)		0.062	0.002	2.30E-04

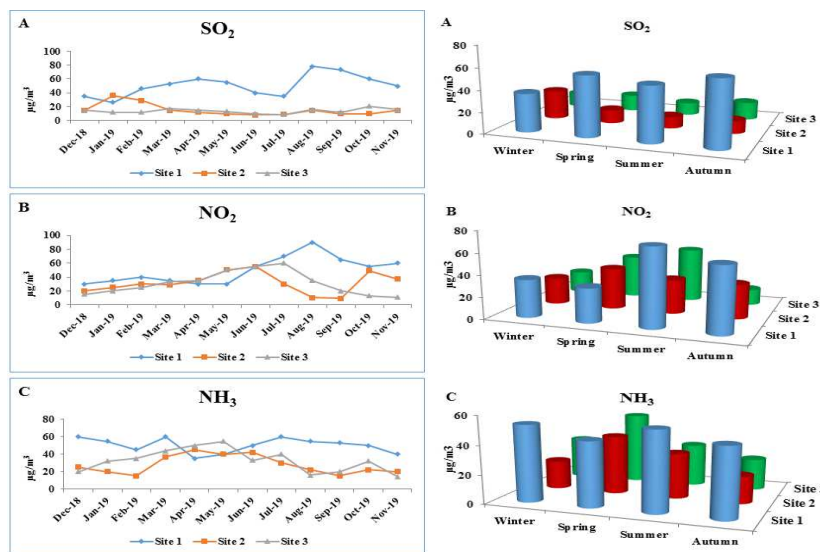


Figure 5: Monthly and Seasonal Means for Some Gaseous Air Pollutants at the Different Investigated Sites (expressed as $\mu\text{g}/\text{m}^3$)

Table 8: Chemical Analysis of Gaseous Air Pollutants at Site (3)

Season	month	SO ₂	NO ₂	NH ₃
Winter	Dec-18	15	15	20
	Jan-19	12	20	32
	Feb-19	12	25	35
Av ± SD		13±1.7	20±5	29±7.9
Spring	Mar-19	17	33	44
	Apr-19	15	35	50
	May-19	13	50	55
Av ± SD		15±2	39.3±9.3	49.7±5.5
Summer	Jun-19	10	55	33
	Jul-19	9	60	40
	Aug-19	16	35	16
Av ± SD		11.7±3.8	50±13.2	29.7±12.3
Autumn	Sep-19	12	20	20
	Oct-19	21	13	32

	Nov-19	16	11	14
Av ± SD	16.3±4.5	14.7±4.7	22±9.2	
Annual mean ± SD	14±3.3	31±16.7	32.6±13.3	
T-Test Sig. (2-tailed)	0.062	0.002	2.30E-04	

Table 9: Correlation Coefficient Values of The Relationships Between The Gases Collected At The Different Studied Sites

Ite m	Site 1			Site 2			Site 3		
	SO ₂	NO ₂	NH ₃	SO ₂	NO ₂	NH ₃	S O ₂	N O ₂	N H ₃
SO ₂	1	0.459	-0.247	1	.601*	0.2	1	0.3	-0.5
NO ₂	0.459	1	0.258	-0.601*	1	0.57	-0.3	1	0.56
NH ₃	-0.247	0.258	1	-0.2	0.57	1	-0.5	0.56	1

*. Correlation is significant at the 0.05 level (2-tailed).

Discussion:**Dust-fall:**

The deposition of atmospheric dust particles by dry or wet deposition is continuous processes. Dust deposition rates are affected by many factors such as dust concentration in the atmosphere, energy of dust transporting winds, and characteristics of depositional environment. Additionally, type and distance of emission sources, location of sampling site, and certain meteorological conditions are some of the other factors involved [23], [24].

The annual means of deposited dust varied between 65.74 ± 60.52 and 78.28 ± 8.45 g/m²/month for studied sites; with the highest rate of 221.28 g/m²/month recorded in October collected at site 1. This rate of deposition is considered very heavy. These surprisingly high dust-fall values in this study also indicate that more effort will be needed to decrease the primary dust-fall emissions, as well as control the formation of secondary pollutants.

Furthermore, these rates exceed the standard for dust deposition in many countries. For example, the air quality standard for the residential areas in USA is 5.7 g/m²/month and is 1.93 g/m²/month as a background value [17]. Nevertheless, dust-fall have no Air Quality Limit value. However, some countries normally state that when dust-fall values exceed 10 g/m² per 30 days, the area may be considered unclean (polluted area) [25].

Moreover, Tables 2, 4 and 6 showed that the rate of dust-fall reached the maximum values in autumn season in all studied locations during the period of study, and then comes winter and spring seasons and the lowest concentrations were recorded in summer. This could be attributed to many factors such as rainfall, light and wind speed that might also have effects. While, the high temperature low relative humidity and active winds may enhance high rate for dust-fall and passage Khamasin dust may cause the high deposition rate in spring. In a previous study in the Gansu Province of China, Ta et al., (2004) reported the highest dust deposition rates values in the spring and the lowest in the autumn [26]. These authors found a positive and significant correlation between dust deposition rates and dust storms but an inverse correlation between dust deposition rates and precipitation [26]. Al-Dousari and AlAwadhi, (2012) investigated the dust deposition rates in northern Kuwait and reported higher quantities of dust deposition rates in November-January, April, July-August and September [27].

Previous research of Chai et al. (2014) shows that particulate matter concentrations in some northern cities in China reached as high as 80–100, while those in the south were 40–70 [28]. It is evident that the

higher values in northern cities are mainly due to the enhanced concentration in winter, while PMs begin to decrease after reaching their maximum value in autumn in southern cities. With insufficient photochemical promotion in winter, the stronger emission of primary particles during the heating period may play a very important role in causing heavy PM pollution.

The concentrations of the total water-soluble matter (TSM) in total deposits were shown in tables 2, 4 and 6 for the investigated sites. Besides, the concentration of TSM varied from one month to another with a slightly higher concentration during autumn then followed by winter. SO_4^{2-} , Cl^- and NH_4^+ were the most important soluble salts measured in dust samples and their concentrations were higher in summer for samples collected from site 1 (Fig. 2-4). While, in sites 2 and 3 the highest concentrations were recorded in winter and/or autumn; which may be likely caused by high fuel consumption due to domestic heating in winter, and more traffic during these periods of the year at investigated sites. These results come in agree with Tan et al., (2017) they stated that traffic emissions is characterized by high levels of water-soluble inorganic ions [29]. Previous studies confirmed that OC and EC were the most abundant species in vehicle exhausts [31–34].

Furthermore, the secondary aerosol formation is characterized by high levels of NH_4^+ , SO_4^{2-} , NO_3^- and Cl^- .

The secondary aerosol accounted for 33% PM_{2.5} mass in winter and 15% in summer. This is likely associated with SO_2 and NO_x emissions from coal combustion and vehicle exhaust forming sulfate and nitrate through photochemical reactions. Although photo-oxidation rates of NO_x and SO_2 are slower in winter than in summer, stationary meteorological conditions and higher levels of gaseous precursors enhanced the levels of secondary inorganic components in winter [29], [34].

In our study, the concentration of nitrates showed a slight seasonal variation with higher values recorded during winter, autumn and summer seasons for studied sites respectively. The relative percentage of nitrates at the investigated sites is mainly due to emission of nitrogen oxides (NO_x) which intern converted to nitrates.

However, the highest average concentrations of insoluble matter were recorded during spring and winter seasons. While the maximum monthly mean was recorded in January for sites 1 and 2 and in May for site 3. These months are characterized by passage of sand storms over Egyptian countries and carry with them desert sands that contains insoluble compounds.

The concentration of Pb and Cd were higher in spring season in site 1; they increased by 1.7 and 8.4 times for Pb and Cd respectively, from spring to summer. While, for the two other sites the highest concentrations were recorded in winter season that increased by 3.1, 0.98, 1.5 and 1.4 times for Pb and Cd in sites 2 and 3 respectively. Such increase could be due to winter domestic heating and stagnant meteorological conditions.

Several emission factors including biomass burning from agricultural fields, sea salt and domestic cooking. As agricultural and domestic areas, biomass burning is common in this region. Thus, biomass-burning emission couldn't be ignored and might be collinear with other sources. All of these factors with traffic and industrial emissions may cause the elevated levels of total deposited matter and its contents of soluble and insoluble components in sites under investigations.

Gaseous Pollutants:

Sulphur dioxide, nitrogen dioxide and ammonia are the major gaseous pollutants in industrial and urban areas. The maximum SO₂ concentrations in our study were recorded in winter and autumn while, lower concentration was recorded in summer (except for site 1) and this may be attributed to climatic conditions, topography and presence of oxidants in the atmosphere. In addition, the low temperature and wind directions during these seasons may enhance the accumulation of SO₂ in the atmosphere. This findings is in agree with Chai et al., (2014), they found that high concentrations of SO₂, and CO were observed in northern cities, especially in winter, indicating strong emissions from coal and biomass or biofuel burning during the heating period[28].

The maximum seasonal concentrations of NO₂ recorded in summer and autumn, additionally, the highest concentration of NO₂ was recorded in site 1 (industrial area) followed by site 3 (traffic-residential area). Such increase may be due to the transport of NO₂ from the pollution source (industrial sector and the traffic emission) by the prevailing wind during these periods of the year. These findings disagreed with Chai et al., (2014); they found that NO₂ dominated the major pollutants in winter, which implies that highly oxidized secondary pollutants were playing a very important role[28]. According to the statistics of major pollution in northern cities, the pollution status was much more complicated in that almost all the pollutants on the list could have been the major pollutant. The NO₂ is a little higher in northern China, which is partly due to residential emissions during the heating period.

The maximum seasonal mean of NH₄ concentrations were recorded in summer and spring

of investigated sites while, the minimum seasonal means were recorded in autumn for all studied sites.

The pattern of autumn and summer high concentrations is mainly attributed to the more intense solar radiation and higher temperatures often associated with the presence of weak, slow-moving, and persistent high-pressure systems, which favor the photochemical oxidation. Thus, the elevated levels observed in the summer and autumn could be explained by the impact of the photochemical process that occurs in the boundary layer. While, the lower concentrations recorded in winter could be attributed to less impact of photochemical pollution in winter, with a decrease of solar radiation and temperature and a reduction in photochemical production [35].

The studied contaminants showed several temporal variations that also observed by earlier studies of Yu et al., (2019) in the urban air of Yangtze River Delta (China), [36], Van Der Wal and Janssen, (2000) in the ambient air of Netherlands [37], and Marcazzan et al., (2001) in atmospheric air of Milan (Italy) [38]. Such differences is due to differences in source of emissions and meteorological situations of each case.

Conclusion:

This article has reported the spatial and seasonal variations of gaseous pollutants (SO₂, NO₂, and NH₃) and dust-fall (soluble and insoluble components) observed in three investigated sites from December 2018 to November 2019. This will help to gain a deeper understanding of the pollution levels of different pollutants, evaluate the attainment of air quality standards, and mark the major pollutants in different seasons at the investigated sites. The surprisingly high dust-fall values in this study also indicate that more effort will be needed to decrease the primary PM emissions, as well as control the formation of secondary pollutants.

Conflicts of interest:

There are no conflicts to declare or personal relationships that could influence the work reported in this paper.

Formatting of funding sources

There was no funding for this research.

References:

- [1] A. K. Haritash and C. P. Kaushik, "Assessment of Seasonal Enrichment of Heavy Metals in Respirable Suspended Particulate Matter of a Sub-Urban Indian City," *Environ. Monit. Assess.*, vol. 128, no. 1–3, pp. 411–420, May 2007.
- [2] R. Bakiyaraj and D. Ayyappan, "air pollution

- tolerance index of some terrestrial plants around an industrial area," *Int. J. Mod. Res. Rev.*, vol. 2, no. 1, pp. 1–7, Jan. 2014.
- [3] M. P. Choudhary and V. Garg, "Causes, Consequences and Control of Air Pollution," in *All India Seminar on Methodologies for Air Pollution Control*: Malviya National Institute of Technology, Jaipur, Rajasthan, India, 2013.
- [4] N. Joshi, A. Chauhan, and P. C. Joshi, "Impact of industrial air pollutants on some biochemical parameters and yield in wheat and mustard plants," *Environmentalist*, vol. 29, no. 4, pp. 398–404, Nov. 2009.
- [5] P. C. Joshi and A. Swami, "Physiological responses of some tree species under roadside automobile pollution stress around city of Haridwar, India," *Environmentalist*, vol. 27, no. 3, pp. 365–374, Jul. 2007.
- [6] N. Zhao et al., "Polymorphisms in oxidative stress, metabolic detoxification, and immune function genes, maternal exposure to ambient air pollution, and risk of preterm birth in Taiyuan, China," *Environ. Res.*, vol. 194, Mar. 2021.
- [7] B. E. Daresta, F. Italiano, G. De Gennaro, M. Trotta, M. Tutino, and P. Veronico, "Atmospheric particulate matter (PM) effect on the growth of *Solanum lycopersicum* cv. Roma plants," *Chemosphere*, vol. 119, pp. 37–42, Jan. 2015.
- [8] A. A. Shaltout, M. M. Gomma, and M. W. Ali-Bik, "Utilization of standardless analysis algorithms using WDXRF and XRD for Egyptian iron ore identification," *X-Ray Spectrom.*, vol. 41, no. 6, pp. 355–362, Nov. 2012.
- [9] A. A. Shaltout, B. Welz, and I. N. B. Castilho, "Determinations of Sb and Mo in Cairo's dust using high-resolution continuum source graphite furnace atomic absorption spectrometry and direct solid sample analysis," *Atmos. Environ.*, vol. 81, pp. 18–24, Dec. 2013.
- [10] A. A. Shaltout, M. A. Allam, N. Y. Mostafa, and Z. K. Heiba, "Spectroscopic Characterization of Dust-Fall Samples Collected from Greater Cairo, Egypt," *Arch. Environ. Contam. Toxicol.*, vol. 70, no. 3, pp. 544–555, Apr. 2016.
- [11] I. N. B. Castilho et al., "Comparison of three different sample preparation procedures for the determination of traffic-related elements in airborne particulate matter collected on glass fiber filters," *Talanta*, vol. 88, pp. 689–695, Jan. 2012.
- [12] D. C. Snyder et al., "Spatial variability of carbonaceous aerosols and associated source tracers in two cities in the Midwestern United States," *Atmos. Environ.*, vol. 44, no. 13, pp. 1597–1608, Apr. 2010.
- [13] P. S. Gilmour et al., "Pulmonary and systemic effects of short-term inhalation exposure to ultrafine carbon black particles," *Toxicol. Appl. Pharmacol.*, vol. 195, no. 1, pp. 35–44, Feb. 2004.
- [14] Z. Liu, B. Hu, L. Wang, F. Wu, W. Gao, and Y. Wang, "Seasonal and diurnal variation in particulate matter (PM₁₀ and PM_{2.5}) at an urban site of Beijing: analyses from a 9-year study," *Environ. Sci. Pollut. Res. Int.*, vol. 22, no. 1, pp. 627–42, Jan. 2015.
- [15] B. Kończak, M. Cempa, Ł. Pierzchała, and M. Deska, "Assessment of the ability of roadside vegetation to remove particulate matter from the urban air," *Environ. Pollut.*, vol. 268, p. 115465, Jan. 2021.
- [16] WHO, "WHO global air quality guidelines," *Coast. Estuar. Process.*, pp. 1–360, 2021.
- [17] A. C. Stern, *Air pollution*, Vol. III., New York: Academic Press Inc., 1986.
- [18] R. M. Harrison and R. Perry, *Handbook of Air Pollution Analysis*, Second Edition. Chapman and Hall, London, New York: Springer Netherlands, 1986.
- [19] M. B. Jacobs and S. Hochheiser, "Continuous Sampling and Ultramicrodetermination of Nitrogen Dioxide in Air," *Anal. Chem.*, vol. 30, no. 3, pp. 426–428, Mar. 1958.
- [20] M. Katz, "theoretical foundations of guidance," *ETS Res. Bull. Ser.*, vol. 1969, no. 1, pp. i–25, Jun. 1969.
- [21] H. Jeong, J. Park, and H. Kim, "Determination of NH₄⁺ in Environmental Water with Interfering Substances Using the Modified Nessler Method," *J. Chem.*, vol. 2013, pp. 1–9, 2013.
- [22] G. C. West, P. W. Gaek, "Fixation of sulfur dioxide as disulphitechloromercurate (II) and subsequent colorimetric estimation," in *Anal. Chem.*, 2nd ed., New York, London: Academic Press, 1956, pp. 1816–1819.
- [23] C. R. Lawrence and J. C. Neff, "The contemporary physical and chemical flux of aeolian dust: A synthesis of direct measurements of dust deposition," *Chem. Geol.*, vol. 267, no. 1–2, pp. 46–63, Sep. 2009.
- [24] S. Norouzi, H. Khademi, S. Ayoubi, A. F. Cano, and J. A. Acosta, "Seasonal and spatial variations in dust deposition rate and concentrations of dust-borne heavy metals, a case study from Isfahan, central Iran," *Atmos. Pollut. Res.*, vol. 8, no. 4, pp. 686–699, 2017.
- [25] B. Sivertsen, A. Aboud, E. Seoud, H. Fathy, and

- H. Ahmed, "Air Pollution in Egypt," no. August, pp. 26–31, 2001.
- [26] W. Ta et al., "Measurements of dust deposition in Gansu Province, China, 1986-2000," *Geomorphology*, vol. 57, no. 1–2, pp. 41–51, 2004.
- [27] A. M. Al-Dousari and J. Al-Awadhi, "Dust fallout in northern Kuwait, major sources and characteristics," *Kuwait J. Sci. Eng.*, vol. 39, no. 2 A, pp. 171–187, 2012.
- [28] F. Chai et al., "Spatial and temporal variation of particulate matter and gaseous pollutants in 26 cities in China," *J. Environ. Sci. (China)*, vol. 26, no. 1, pp. 75–82, Jan. 2014.
- [29] J. Tan et al., "Chemical characteristics and source apportionment of PM_{2.5} in Lanzhou, China," *Sci. Total Environ.*, vol. 601–602, pp. 1743–1752, Dec. 2017.
- [30] Y. Wang et al., "Chemical characterization and source apportionment of PM_{2.5} in a semi-arid and petrochemical-industrialized city, Northwest China," *Sci. Total Environ.*, vol. 573, pp. 1031–1040, Dec. 2016.
- [31] X. Wang, Y. Nie, H. Chen, B. Wang, T. Huang, and D. Xia, "[Pollution Characteristics and Source Apportionment of PM_{2.5} in Lanzhou City]," *Environ. Sci.*, vol. 37, no. 5, pp. 1619–28, May 2016.
- [32] J. Tao, L. Zhang, J. Cao, and R. Zhang, "A review of current knowledge concerning PM_{2.5} chemical composition, aerosol optical properties and their relationships across China," *Atmos. Chem. Phys.*, vol. 17, no. 15, pp. 9485–9518, 2017.
- [33] J. Tao et al., "Source apportionment of PM_{2.5} at urban and suburban areas of the Pearl River Delta region, south China - With emphasis on ship emissions," *Sci. Total Environ.*, vol. 574, pp. 1559–1570, 2017.
- [34] F. W. Lurmann, S. G. Brown, M. C. McCarthy, and P. T. Roberts, "Processes influencing secondary aerosol formation in the San Joaquin valley during winter," *J. Air Waste Manag. Assoc.*, vol. 56, no. 12, pp. 1679–1693, 2006.
- [35] J. A. Logan, "Ozone in rural areas of the United States," *J. Geophys. Res. Atmos.*, vol. 94, no. D6, pp. 8511–8532, Jun. 1989.
- [36] Y. Yu, J. Wang, J. Yu, H. Chen, and M. Liu, "Spatial and temporal distribution characteristics of PM_{2.5} and PM₁₀ in the urban agglomeration of China's Yangtze river delta, China," *Polish J. Environ. Stud.*, vol. 28, no. 1, pp. 445–452, 2019.
- [37] J. T. Van Der Wal and L. H. J. M. Janssen, "Analysis of spatial and temporal variations of PM₁₀ concentrations in the Netherlands using Kalman filtering," *Atmos. Environ.*, vol. 34, no. 22, pp. 3675–3687, 2000.
- [38] G. M. Marazzan, S. Vaccaro, G. Valli, and R. Vecchi, "Characterisation of PM₁₀ and PM_{2.5} particulate matter in the ambient air of Milan (Italy)," *Atmos. Environ.*, vol. 35, no. 27, pp. 4639–4650, 2001.